Research Article

Journal of MASS SPECTROMETRY

Received: 11 September 2009 Accepted: 16 November 2009 Published online in Wiley Interscience:

(www.interscience.com) DOI 10.1002/jms.1709

Fully automated liquid extraction-based surface sampling and ionization using a chip-based robotic nanoelectrospray platform†

Vilmos Kertesz* and Gary J. Van Berkel*

A fully automated liquid extraction-based surface sampling device utilizing an Advion NanoMate chip-based infusion nanoelectrospray ionization system is reported. Analyses were enabled for discrete spot sampling by using the Advanced User Interface of the current commercial control software. This software interface provided the parameter control necessary for the NanoMate robotic pipettor to both form and withdraw a liquid microjunction for sampling from a surface. The system was tested with three types of analytically important sample surface types, *viz.*, spotted sample arrays on a MALDI plate, dried blood spots on paper, and whole-body thin tissue sections from drug dosed mice. The qualitative and quantitative data were consistent with previous studies employing other liquid extraction-based surface sampling techniques. Published in 2009 by John Wiley & Sons, Ltd.

Supporting information may be found in the online version of this article.

Keywords: surface sampling; nanoelectrospray; mass spectrometry; dried blood spots; thin tissue sections; MALDI spots

Introduction

One segment of our research on ambient surface sampling and ionization techniques for use with mass spectrometry (MS)[1–3] has focused on the understanding and advancement of what we call a liquid microjunction surface sampling probe (LMJ-SSP) (Fig. 1).[4–14] Reported applications of the LMJ-SSP include sampling and analysis of dried drugs or proteins or solutions thereof from wells on microtiter plates,[4] drugs captured in solid-phase extraction cards,[6] dyes, inks or pharmaceuticals on paper or separated on hydrophobic reversed-phase (C8 and C18) thin-layer chromatography plates,[5,7–10]exogenous compounds from thin tissue sections,[13,14] and surface deposited and affinity captured proteins.[12] The LMJ-SSP has also been configured as a two-electrode electrochemical cell to enable analytically beneficial electrochemically initiated analyte modifications.[15]

The LMJ-SSP is typically used as a liquid-solid extraction system to directly reconstitute or extract an analyte from a surface by connecting the probe and surface via a wall-less 'liquid microjunction'. To do this the LMJ-SSP systems have been configured so that the extracting liquid is both brought to the surface and is then carried on to the ionization source through a probe acting as a liquid conduit. The solvent flow rate into the probe is balanced by the liquid aspiration rate of the sampling probe induced by a pneumatically assisted electrospray ionization (ESI) or atmospheric pressure chemical ionization (APCI) emitter. Thus, this surface sampling probe can be applied to all species that can be dissolved in the liquid flowing through the probe and subsequently ionized by the chosen ionization method. In this configuration, the LMJ-SSP can operate in either a discrete spot sampling (profiling) mode or an imaging mode.[13]

A key step in the use of the LMJ-SSP probe is the formation of the probe-to-surface liquid microjunction.[5] With respect to discrete spot sampling, we recently demonstrated a simple and relatively fast (30 s sample-to-sample) automated method for both formation and withdrawal of the liquid microjunction.[16] With the probe positioned at an appropriate distance from the surface (typically about 200 μm), a liquid microjunction was formed by allowing the liquid from the sampling end of the probe to extend out from the probe to touch the surface. Species on the surface that dissolved in the liquid were drawn back into the probe and electrosprayed. The control over liquid flow to and from the surface was accomplished by altering the self-aspiration liquid flow rate out of the probe by changing the nebulizing gas flow rate.

Importantly, it was recognized that this new high-throughput discrete spot sampling mode was not restricted to the continuous flow design of the LMJ-SSP. Rather, this sampling mode might be implemented with any 'probe' capable of both dispensing and retrieving the solution from the surface. In addition, having the method available as part of a current commercially available, automated system has the significant advantage to further advance the area of ambient surface sampling. In this paper, we show that the commercially available Advion NanoMate chip-based infusion nanoESI system[17–20] can be adapted to perform in a fully automated fashion this type of discrete spot sampling with subsequent mass spectrometric analysis. Presented here is a procedure for implementing the experiment using the current Advanced User Interface (AUI) of the NanoMate ChipSoftManager software. To illustrate the utility of the approach, three types of

* *Correspondence to: Vilmos Kertesz and Gary J. Van Berkel, Organic and Biological Mass Spectrometry Group, Chemical Sciences Division, Oak Ridge National Laboratory, Oak Ridge, TN 37831-6131, USA.*
E-mail: kerteszv@ornl.gov; vanberkelgj@ornl.gov

Organic and Biological Mass Spectrometry Group, Chemical Sciences Division, Oak Ridge National Laboratory, Oak Ridge, TN 37831-6131, USA

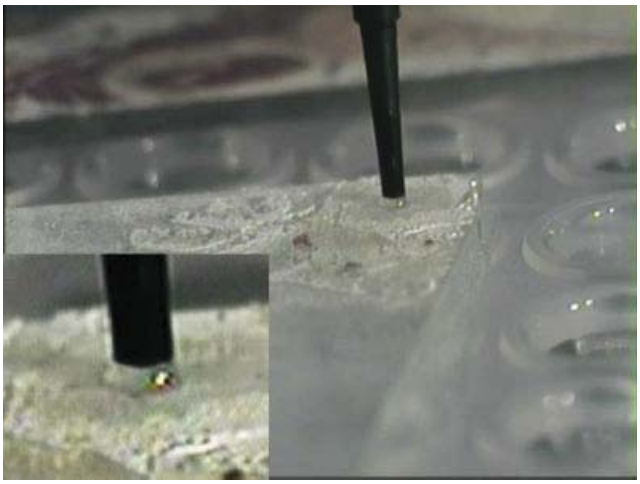

Figure 1. Far and (inset) magnified views of a liquid microjunction created between the robotically controlled pipette tip and a brain thin tissue section.

analytically important sample surface types were analyzed, *viz*., spotted sample arrays on a MALDI plate, dried blood spots on paper and whole-body thin tissue sections from drug dosed mice. Data are presented from the quantitative analysis of verapamil spotted for MALDI along with the MALDI matrix, the quantitative analysis of sitamaquine in dried blood spots, and the detection and semiquantitative analysis of two different drugs (propranolol and sulforaphane) and their respective metabolites in organs within whole-body thin tissue sections from the drug dosed mice. Figures-of-merits reported include sampling spot size, spot-to-spot sampling speed, signal reproducibility, linear dynamic range and sample carryover. Comparisons are made between these data and our reported results analyzing the same samples with the conventional LMJ-SSP[13,14,16] and with a sealing surface sampling probe system (SSSP).[21]

Experimental Section

Chemicals

High performance liquid chromatography (HPLC) grade acetonitrile (ACN), methanol (MeOH) and water were purchased from Burdick & Jackson (Muskegon, MI, USA). Formic acid (FA) (≥96% purity) was purchased from Sigma-Aldrich (St Louis, MO, USA). Verapamil hydrochloride (Acros Organics, Morris Plains, NJ, USA), propranolol hydrochloride (Acros Organics), alpha cyano-4-hydroxycinnamic acid (CHCA, Sigma-Aldrich), and R,S-sulforaphane (LKT Laboratories, Inc., St Paul, MN, USA) were obtained commercially and used without further purification. Sitamaquine [*N*,*N*-diethyl-*N*-(6-methoxy-4-methylquinolin-8-yl)hexane-1,6-diamine] and stable isotopically labeled internal standard, sitamaquine-d10 dihydrochlorides were obtained from GlaxoSmithKline (Greenford, UK and Isotope Chemistry, Stevenage, UK, respectively).

MALDI spots

MALDI matrix solution was prepared by dissolving CHCA in a mixed solvent containing 58/34/8 (v/v/v) ACN/MeOH/water at a final concentration of 12 mg/ml unless otherwise stated. Verapamil and propranolol stock solutions were prepared in the mixed solvent of 58/34/8 (v/v/v) ACN/MeOH/water. The MALDI matrix solution was mixed with the analyte stock solutions prior to spotting to obtain the required verapamil (1–200 ng/ml), propranolol (200 ng/ml) and CHCA (1.5 mg/ml) concentrations. Sample aliquots (0.5 μl) were spotted with a variable volume (0.5–2.5 μl) pipette onto and analyzed from an ABI stainless steel Opti-TOF 96 well plate insert (Applied Biosystems, Carlsbad, CA, USA).

Dried blood spots

Stock solutions (1 mg/ml) of sitamaquine and sitamaquine-d10 were prepared in 50/50 (v/v) MeOH/water. Rat blood was mixed with the analyte stock solutions prior to spotting to obtain the required sitamaquine (10–10 000 ng/ml) and sitamaquine-d10 (570 ng/ml) concentrations. Aliquots (15 μl) of the dosed rat blood samples were spotted onto Ahlstrom 237 filter paper (Ahlstrom Corp., Helsinki, Finland), for both the calibration standards and quality control samples, and allowed to dry at room temperature for at least 2 h. Samples were stored desiccated at 4 °C until use. Disks 4 mm in diameter were punched from the center of the dried blood spots and secured onto an ABI stainless steel Opti-TOF 96 well plate insert using double-sided tape (3M, St Paul, MN, USA).

Thin tissue sections

In the propranolol related studies, male CD-1 mice (Charles River Laboratories) were administered propranolol intravenously via the tail vein at 7.5 mg/kg as an aqueous solution in 0.9% NaCl. At 60-min post-dose, mice were euthanized with an isoflurane overdose and immediately frozen in dry ice/hexane. In the sulforaphane related studies, male C57BL/6 mice (Charles River Laboratories) were administered sulforaphane at 90 mg/kg (as an aqueous solution) by oral gavage. At 3-h post-dose, mice were euthanized in a carbon dioxide chamber and immediately frozen in dry ice/hexane. The frozen mice were embedded/blocked in 2% aqueous carboxymethyl cellulose. Sagittal whole-body cryosections (40-μm thick) were prepared using a Leica CM3600 cryomacrotome. Frozen sections were transferred to 3″ × 4″, 1.2-mm thick glass slides (Brain Research Laboratories) using a tape transfer process (Macro-Tape-Transfer System®, Instrumedics, St Louis, MO, USA), which utilizes a photoactivated polymer adhesive. After transfer to the glass slides, the sections were freeze-dried within the cryomacrotome chamber. All tissue sections were stored in a desiccator at room temperature until analysis. The tissue sections dosed with sulforaphane or propranolol were approximately 3.5 years and 2 months old, respectively. Color images of the tissue sections were acquired using a HP Scanjet 4370 flat-bed scanner (Hewlett-Packard, Palo Alto, CA, USA). Coregistration of the optical images and the surface spots sampled was accomplished manually.

Automated liquid extraction-based surface sampling

All samples were analyzed using a NanoMate 100 system (Advion BioSciences, Inc. Ithaca, NY, USA) coupled to a 4000 QTRAP® mass spectrometer (MDS SCIEX, Concord, Ontario, Canada). A nanoelectrospray voltage of 1.55 kV and gas pressure of 0.2 psi was applied in all experiments. Scheme 1 shows the compound structures and the monitored precursor and product ions. Mass spectrometer parameters used for specific analytes are summarized in Table 1. Customized robotic arm movements and custom liquid handling for a surface analysis was setup in the AUI panel of the ChipSoftManager software controlling the NanoMate.

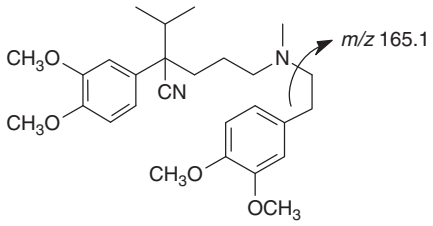

verapamil

$(M + H)^+ = m/z$ 455.3

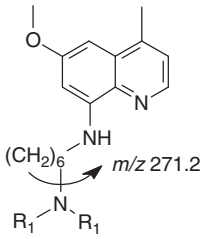

sitamaquine (R_1=C_2H_5)

$(M + H)^+ = m/z$ 344.4

sitamaquine-d10 (R_1=C_2D_5)

$(M + H)^+ = m/z$ 354.4

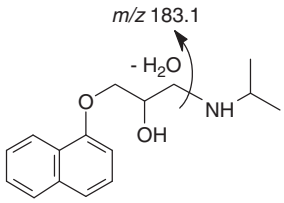

propranolol

$(M + H)^+ = m/z$ 260.1

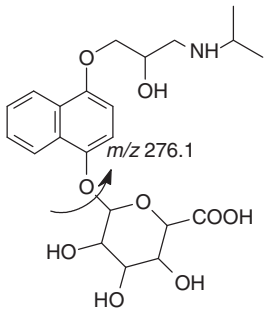

4-hydroxypropranolol glucuronide

$(M + H)^+ = m/z$ 452.1

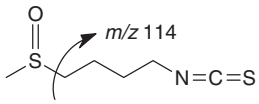

sulforaphane

$(M + H)^+ = m/z$ 178.1

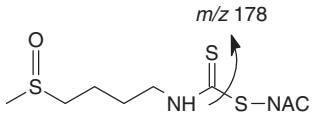

sulforaphane *N*-acetyl cysteine (NAC) conjugate

$(M + H)^+ = m/z$ 341

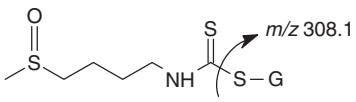

sulforaphane glutathione (G) conjugate

$(M+H)^+ = m/z$ 485.1

Scheme 1. Structure and mass-to-charge ratio of analytes and origin of major product ions.

Results and Discussion

Liquid extraction-based surface sampling using the NanoMate platform

To better explain the operation of the NanoMate platform for surface sampling we first will describe the normal automated operation of the device for infusion nanoESI.[17–20] Solutions of the samples to be analyzed are loaded into a well plate that is placed in the device. A robotic arm picks up a conductive pipette tip and moves the tip to a position above a specific sample well. The pipette tip is lowered into the well and a specific volume of sample is aspirated into the pipette tip. Then the robotic arm withdraws from the well and engages the pipette tip to the back of the ESI chip. This chip contains microfabricated nozzles to generate nanoESI of liquid samples at flow rates of 20–500 nl/min. The nanoelectrospray is initiated by applying the appropriate high voltage to the pipette tip and gas pressure on the liquid. Each nozzle and pipette tip is used only once to eliminate any possibility of sample-to-sample carryover.

Table 1. Analytes, SRM transitions and parameter settings including declustering potential (DP) and collision energy (CE)

Analyte	Q1 (*m/z*)	Q3 (*m/z*)	DP (V)	CE (eV)
Verapamil	455.3	165.1	100	40
Sitamaquine	344.4	271.2	42	30
Sitamaquine-d10	354.4	271.2	42	30
Sulforaphane	178.1	114	110	17
SFN-GSH conjugate	485.1	308.1	60	24
SFN-NAC conjugate	341	178	60	15
Propranolol	260.1	183.1	60	27
Hydroxypropranolol glucuronide	452.1	276.1	60	35

The individual steps involved in using the NanoMate platform for liquid extraction-based surface sampling and subsequent infusion nanoESI-MS are illustrated in Scheme 2. All these steps were automated and accomplished using the AUI panel of the ChipSoftManager software controlling the NanoMate. Prior to the analysis, the particular surface to be analyzed was secured with clear tape onto the top of a typical 96-well plate used in the system. The surface was affixed so that the particular surface positions to be sampled were directly over the normal sampling positions of the 96-well plate. In addition, the surface was positioned so that some sample wells were still accessible for sampling of solution by the robotic pipette tip (see Supporting Information Fig. S1). One or more of these exposed wells was filled with the extraction solvent(s) to be used for the experiment.

To begin the surface sampling process, the robotic arm picked up a conductive pipette tip and moved the tip to a position above the well containing the extraction solvent (Scheme 2a), lowered into the well and solvent was aspirated into the tip (Scheme 2b). Then, the pipette tip was positioned above the surface spot to be sampled and a specific volume of the extraction solvent was dispensed onto the sample from the tip without breaking the liquid junction between the pipette tip and surface (Scheme 2c). Figure 1 shows normal and zoomed-in views of such a liquid microjunction. Typically, the diameter of the junction was slightly larger than the 1-mm diameter of the pipette tip. The distance between the tip and the surface, and the volumes aspirated and dispensed were optimized for each individual surface (see below). Immediately thereafter the solution containing the dissolved sample was aspirated back into the tip (Scheme 2d). In the final step of the surface sampling process, the sample solution was sprayed through a nanospray nozzle (Scheme 2e) while collecting the mass spectrometric response of the analyte of interest using selected reaction monitoring (SRM). It might be expected that the nozzles would be clogged by particulate matter sampled from the surface. Fortunately, this phenomenon was not observed with the three surface types discussed here. This was probably due in part to the use of appropriate solvents and extraction parameters. Extraction solvents and volumes for the different surfaces/analytes and for the different aspirate and dispense steps are summarized in Table 2.

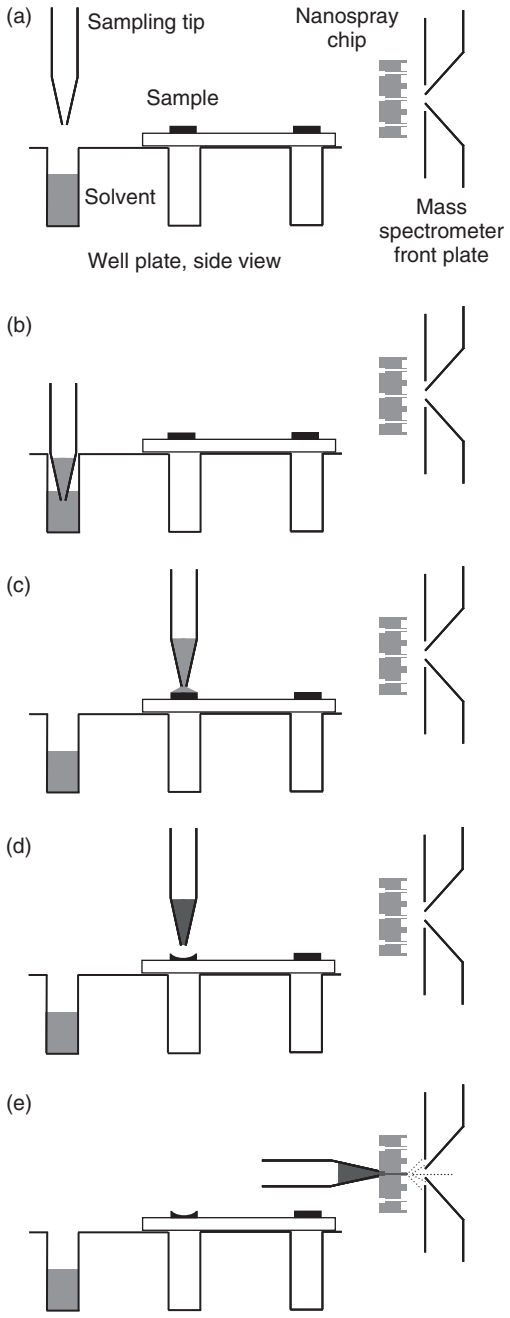

Scheme 2. Individual steps of the surface sampling process.

Analysis of samples prepared for MALDI

Recent advances in MALDI-MS for high-throughput quantitative analysis have resulted in systems capable of analyzing samples at a rate higher than one sample per second.[22–25] However, MALDI, like all other commonly used ionization techniques, is not a universal ionization source. Literature reports have indicated that ~85% of drug-like molecules have sufficient MALDI response to allow routine analysis of samples from DMPK discovery screening assays.[22] The remaining 15% might be successfully analyzed by ESI (or APCI). We recently demonstrated direct ESI analysis of dried MALDI samples using LMJ-SSP/MS.[16] Those results indicated that a liquid extraction-based surface sampling probe could be used to re-assay samples previously analyzed but not completely consumed by MALDI (e.g. spots analyzed using lane scanning) allowing the identical samples to be interrogated by both ESI and MALDI. Analysis of a similar sample set was accomplished with the NanoMate to evaluate the analytical performance of this liquid extraction-based surface sampling probe for such an analysis.

Journal of MASS SPECTROMETRY

Table 2. Samples, extraction solvents and solvent/extract volumes for the different steps of the surface analysis

Sample	Extraction solvent	Volume (µl) of: Aspirated solvent	Dispensed solvent	Aspirated extract
MALDI spots	58/34/8/0.1 (v/v/v/v) ACN/MeOH/H_2O/FA	1.5	1	1
Dried blood spots	58/34/8/0.1 (v/v/v/v) ACN/MeOH/H_2O/FA	4	3	2
Thin tissue sections	80/20/0.1 (v/v/v) ACN/H_2O/FA	3	2	2

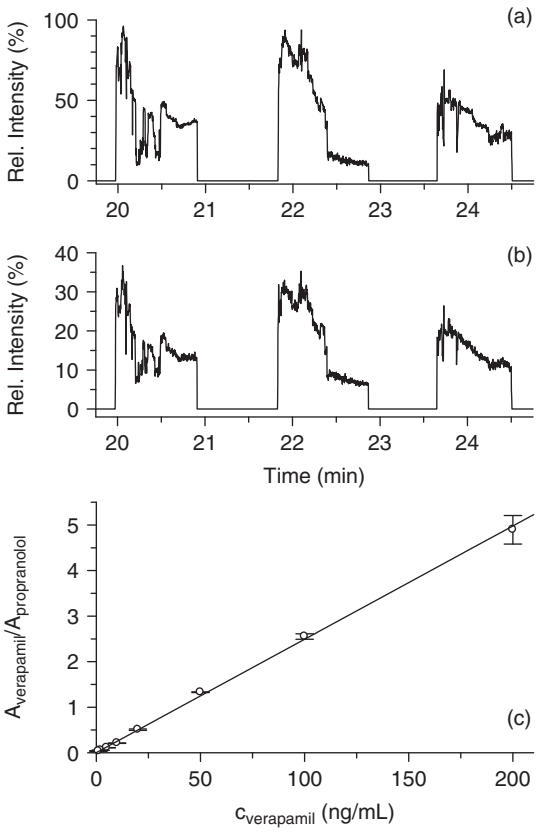

Figure 2. SRM ion current chronograms of (a) verapamil (m/z 455.3 → 165.1, CE=40 eV) and (b) propranolol (m/z 260.1 → 183.1, CE=27 eV) obtained from the sampling of three different spots (0.5 µl deposited) of verapamil (100 ng/ml), propranolol (200 ng/ml) and CHCA matrix (1.5 mg/ml) from a stainless steel MALDI plate insert. Dwell time was 50 ms for each transition monitored. Extraction solvent was 58/34/8/0.1 (v/v/v/v) ACN/MeOH/water/FA. Aspirated and dispensed solvent volumes were 1.5 and 1 µl, respectively, and aspirated sample volume was 1 µl. (c) Average of the ratio of integrated SRM signal of verapamil (1–200 ng/ml) and that of propranolol (200 ng/ml) ($A_{verapamil}/A_{propranolol}$) as a function of verapamil concentration ($c_{verapamil}$) in the spots deposited onto the MALDI plate insert. The data was analyzed using a least-squares regression with a $1/c_{verapamil}$ weighting and fit the model of $A_{verapamil}/A_{propranolol} = 2.29 \times 10^{-2}$ $c_{verapamil} + 8.46 \times 10^{-4}$ ($r^2 = 0.998$). Data from the results shown are summarized in Table 3.

The SRM ion current chronograms of verapamil and propranolol in Fig. 2a, b, respectively, were obtained from the sampling of three different surface spots of the analyte verapamil and propranolol internal standard from a stainless steel MALDI plate insert. Note, that the signal truncation after 1 min of data collection was caused by aborting the spraying process. Inspection of these data showed that the analyte and internal standard did not have quasi-constant signal levels during the 1-min spraying. The spray profiles always exhibited a higher signal region at the beginning and that signal generally decreased over time. The exact reason for this behavior is not understood, but is believed to be related to the nature of the solvent system being used. Conditions that maintain a more consistent spray level might be achieved, but quantitation was possible with the current data.

Table 3. Nominal ($c_{verapamil}$) and calculated mean ($c_{calc,verapamil}$) concentrations, precision (CV%, n=3) and accuracy (bias%) for verapamil in the MALDI spots analyzed

$c_{verapamil}$ (ng/ml)	$c_{calc,verapamil}$ (ng/ml)	Precision (CV%)	Accuracy (bias%)
200	196.6	6.4	−1.7
100	102.4	2.4	2.4
50	53.3	0.6	6.6
20	20.3	3.0	1.5
10	8.35	2.4	−16.5
5	4.25	3.6	−14.9
2	2.11	6.1	5.6
1	1.31	26.3	30.7

Using three replicates at each verapamil concentration, a calibration curve was constructed using the ratio of background corrected integrated SRM signal of verapamil and that of propranolol ($A_{verapamil}/A_{propranolol}$) (over the 1-min spraying period) as a function of verapamil concentration ($c_{verapamil}$). The resulting calibration curve (solid line), the averaged data ($n = 3$, open circles) and associated error bars (CV) obtained are plotted in Fig. 2c. As summarized in Table 3 the precision of measurements (CV) was less than about 7% down to the 2 ng/ml samples, increasing to 26.3% for the 1-ng/ml samples. The back calculated concentrations generally showed an accuracy within 17% down to the 2-ng/ml level. Thus, this method provides the required accuracy, and nearly satisfies the required precision (15%) within internationally recognized acceptance criteria for assay validations[26] down to the 2-ng/ml level.

Similar quantitation performance metrics (<15% precision, ≤17% accuracy down to the 2.5-ng/ml level) were achieved recently for a similar sample set using a LMJ-SSP system.[16] In comparison, the LMJ-SSP method offered higher sample throughput (0.5 min/sample as opposed to about 2 min/sample presented here). However, the NanoMate system inherently provides for carryover-free analysis by using disposable pipette tips to collect and spray the sample.

Dried blood spot analysis

Dried blood spots are an accepted and expedient way to collect, store and ship samples for analysis in neonatal screening.[27–29] They are becoming more utilized for the same reasons in the drug

discovery and clinical environments for applications ranging from pharmacokinetics to therapeutic drug monitoring.[30,31] Currently, to analyze such blood spots, samples are punched, extracted, cleaned up and flow injection or HPLC with tandem MS is used to quantify the targeted analytes. This multiple step analysis process can be completely automated, but the use of a direct surface sampling, ionization and analysis method has the potential to simplify, speed up and cut analysis costs.

Figure 3a, b show the SRM ion current chronograms for sitamaquine and sitamaquine-d10, respectively, obtained from the analysis of three dried blood spot punch replicates. As was the case for the MALDI spots, the analyte and internal standard did not have quasi-constant signal levels. Furthermore, the absolute analyte signals significantly varied between replicates. Again, this variation was believed to be due, at least in part, to the particular solvent system used. In addition, the sampling process from the paper matrix also might have contributed to the analyte signal variation. More specifically, the dried blood spot punches had a significant height difference and were considerably absorbent. For these reasons, analytically best results were achieved when the paper-based punches were slightly 'squeezed' during the sample aspiration step to maximize sample volume aspirated back into the pipette tip. This was accomplished by lowering the pipette tip to push into the surface of the punches. Note, that this type of sampling was different from that used for sampling from a MALDI plate (above) or thin tissue sections (below), which employed simply a liquid microjunction between the surface and the pipette tip.

Using three replicates at each sitamaquine concentration, a calibration curve was constructed using the ratio of background corrected integrated SRM signal of sitamaquine and that of sitamaquine-d10 ($A_{sitamaquine}/A_{sitamaquine-d10}$) (over the 1-min spraying period) as a function of sitamaquine concentration ($c_{sitamaquine}$). The resulting calibration curve (solid line), the averaged data ($n = 3$, open circles) and associated error bars (CV) obtained are plotted in Fig. 3c. As summarized in Table 4 the measurement precision (CV) was better than about 6% down to the 200-ng/ml samples, increasing gradually to 98% for the 10-ng/ml samples. The back calculated concentrations generally showed an accuracy within 15% down to the 100-ng/ml level. Thus, this method provides the required accuracy and precision within internationally recognized acceptance criteria for assay validations[26] down to the 100-ng/ml level.

These quantitation metrics are similar to those achieved recently using a liquid extraction-based SSSP with the same sample set (<15% precision, <15% accuracy down to the 50-ng/ml level).[21] While the sampling speeds of the two techniques were comparable (2.5 min/sample for the SSSP and about 2 min/sample for the NanoMate), the need for a washing step to eliminate carryover with the SSSP contributed significantly to the total analysis time. Because of the SSSP design, complete elimination of sample carryover required extraction at a blank spot (typically 60 s) on the sampling surface (or another blank surface). This procedure ensured cleaning the SSSP plunger face and tubing from the plunger to the valve and on into the ion source. Again, carryover was not an issue with the NanoMate where sample-to-sample analysis time was largely limited by the speed of the robotic system.

Thin tissue section analysis

Whole-body autoradiography (WBA) using radiolabeled drugs are often applied for quantitative chemical imaging of total

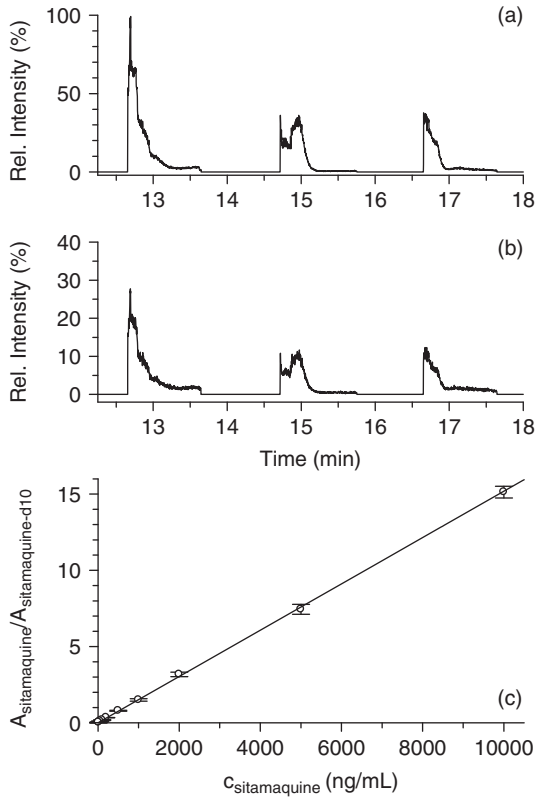

Figure 3. SRM ion current chronograms of (a) sitamaquine (m/z 344.4 → 271.2, CE = 30 eV) and (b) sitamaquine-d10 (m/z 354.4 → 271.2, CE = 30 eV) obtained from the analysis of three 4-mm-diameter dried blood sample punches. Dwell time was 50 ms for each transition monitored. Dried blood samples were prepared by spotting 15 µl rat blood containing 2000 ng/ml sitamaquine and 570 ng/ml sitamaquine-d10 onto Ahlstrom 237 paper. Extraction solvent was 58/34/8/0.1 (v/v/v/v) ACN/MeOH/water/FA. Aspirated and dispensed solvent volumes were 4 and 3 µl, respectively, and aspirated sample volume was 2 µl. (c) Average of the ratio of integrated SRM signal of sitamaquine (10–10 000 ng/ml) and that of sitamaquine-d10 (570 ng/ml) ($A_{sitamaquine}/A_{sitamaquine-d10}$) as a function of sitamaquine concentration ($c_{sitamaquine}$) in the blood spotted onto the paper substrate. The data was analyzed using a least-squares regression with a $1/c_{sitamaquine}$ weighting and fit the model of $A_{sitamaquine}/A_{sitamaquine-d10} = 1.51 \times 10^{-3}\ c_{sitamaquine} + 5.63 \times 10^{-3}$ ($r^2 = 0.999$). Data from the results shown are summarized in Table 4.

Table 4. Nominal ($c_{sitamaquine}$) and calculated mean ($c_{calc,sitamaquine}$) concentrations, precision (CV%, n=3) and accuracy (bias%) for sitamaquine in the dried blood spot punches analyzed

$c_{sitamaquine}$ (ng/ml)	$c_{calc,sitamaquine}$ (ng/ml)	Precision (CV%)	Accuracy (bias%)
10 000	9985.6	2.6	−0.1
5 000	4904.8	4.4	−1.9
2 000	2091.7	4.8	4.6
1 000	985.1	5.3	−1.5
500	513.8	4.3	2.8
200	218.9	4.3	9.5
100	113.6	13.4	13.6
50	62.4	25.6	24.7
20	9.57	45.7	−52.1
10	17.8	98.0	77.7

Journal of MASS SPECTROMETRY

drug-related compounds in thin tissue sections.[32] However, this technique does not distinguish between the parent drug and the metabolites. Punched samples from these same sections or whole organ tissue homogenates are used with conventional sample extraction, cleanup and HPLC-MS or MS/MS to identify and quantify particular molecular forms of the drug-related material present. As with the dried blood spots, this procedure might be fully automated but a direct surface sampling, ionization and analysis method could save time and other resources.

Tissues dosed separately with two different drugs were examined. First, a whole-body thin tissue section from a mouse that had been administered sulforaphane was analyzed. The areas sampled are annotated in the photograph of the tissue shown in Fig. 4a. The SRM chronograms obtained for sulforaphane and its glutathione (SFN-GSH) and *N*-acetylcystine (SFN-NAC) metabolites from the sequential sampling of the different organs are shown in Fig. 4b–d, respectively. Note that with this solvent system and sample type, the SRM signal levels were consistent over the complete 1-min analysis time for each spot analyzed. SFN-GSH conjugate had the highest signals for stomach (spot 1) and somewhat lower levels in the stomach wall (spots 3 and 4). This suggests a high level of unabsorbed SFN after oral administration at this dose. The two compounds were not detected in the kidney or liver tissues (spots 2 and 5, respectively). On the other hand, NAC conjugate of sulforaphane was readily detected in the liver and kidney (spots 2 and 5, respectively), and only background level signals were recorded for the stomach and stomach walls (spots 1, 3 and 4, respectively). For comparison, results from the analysis of the control tissue are presented in Fig. S2. In general, these observations made are in line with the previously reported LMJ-SSP-MS/MS analysis[13] of tissues from the same mouse.

The second whole-body thin tissue section examined was from a mouse that had been administered propranolol. The areas sampled are marked in the optical image of the tissue shown in Fig. 5a. The SRM chronograms recorded for propranolol and its hydroxypropranolol glucuronide metabolite from the sampling of the different organs are shown in Fig. 5b, c, respectively. Again, SRM signal levels were consistent over the complete 1-min analysis time for each spot analyzed. Propranolol was detected in all organs examined. Relatively higher signals levels were for stomach, kidney and muscle (spots 3, 4 and 6, respectively), somewhat lower signals for lung and brain (spots 1 and 5, respectively) and lowest for liver (spot 2). Signal levels for hydroxypropranolol glucuronide were highest in the liver and kidney (spots 2 and 4, respectively). Glucuronidation occurs mainly in the liver, making the drug more water-soluble to enhance subsequent elimination from the body by urination via the kidneys.[33] Lower hydroxypropranolol glucuronide signal was observed in the lung (spot 1) and this metabolite was not detected in the stomach, brain and muscle (spots 3, 5 and 6). Sampling the same organs of a control tissue section resulted in lack of signal for both the parent drug and its metabolite (Fig. S3). Again, these general observations are in line with the previously reported SSSP,[21] and LMJ-SSP-MS/MS and WBA analyses[14] of brain, liver, kidney and lung tissues of a mouse dosed following the same protocol as described here.

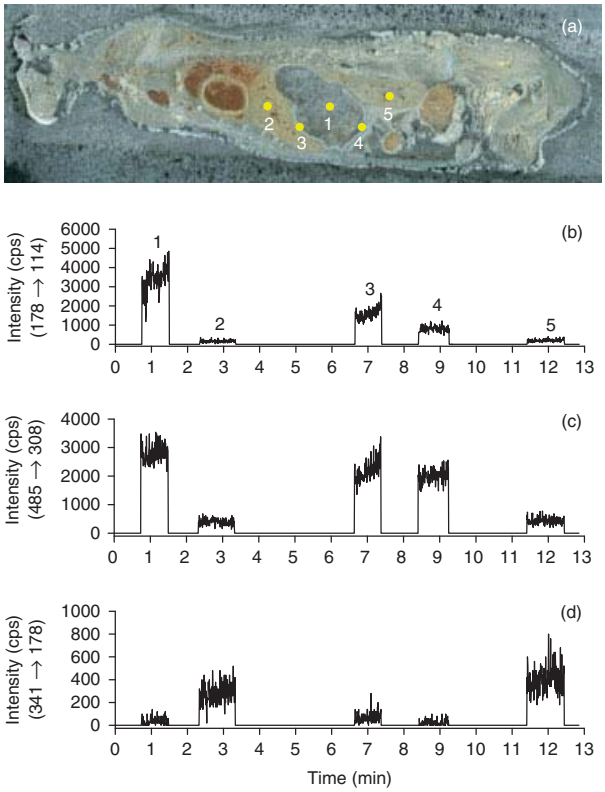

Figure 4. (a) Photograph of a sulforaphane dosed mouse (90 mg/kg, oral gavage, sacrificed 3 h after dose) whole-body thin tissue section showing five discrete points analyzed using the robotic nanospray system. Signal levels for (b) sulforaphane (*m/z* 178 → 114) (c) the GSH conjugate (*m/z* 485 → 308) and (d) the NAC conjugate (*m/z* 341 → 178) were recorded during 1-min spraying of samples taken at each point. Dwell time was 50 ms for each transition monitored. Extraction solvent was 80/20/0.1 (v/v/v) ACN/water/FA. Aspirated and dispensed solvent volumes were 3 and 2 µl, respectively, and aspirated sample volume was 2 µl. Sampling locations: 1 = stomach/contents; 2 = liver; 3 and 4 = wall of stomach; 5 = kidney.

Conclusions

In this paper, we described the use of an Advion NanoMate chip-based infusion nanoESI system for carryover-free, liquid extraction-based surface sampling with subsequent mass spectrometric analysis of the extract. The discrete spot sampling mode demonstrated was implemented using the current hardware and software elements of the NanoMate system. The area sampled was somewhat larger than the 1-mm diameter of the robotic pipette tip used to deliver and retrieve the extraction solvent from the surface. Quantitative analysis of verapamil samples spotted with internal standard (propranolol) and a MALDI matrix compound (CHCA) showed the system could provide acceptable accuracy and precision within internationally recognized acceptance criteria for assay validations, without carryover issues, down to the 2-ng/ml level. Quantitative evaluation of dried blood spots containing a minimum of 100-ng/ml sitamaquine resulted in similarly acceptable data. Two different sets of whole-body thin tissue sections of mice dosed with drug compounds sulforaphane and propranolol were also analyzed. Analyses of the thin tissue sections provided at the minimum a semiquantitative abundance of the targeted drugs and metabolites in the individual organs sampled. These relative abundance data were consistent with previous LMJ-SSP-MS/MS (sulforaphane), and SSSP, LMJ-SSP-MS/MS and WBA studies (propranolol) of tissue sections from mice subjected to the same drug administration protocol.

While the analyses performed here were successful using the hardware and software elements already present in the

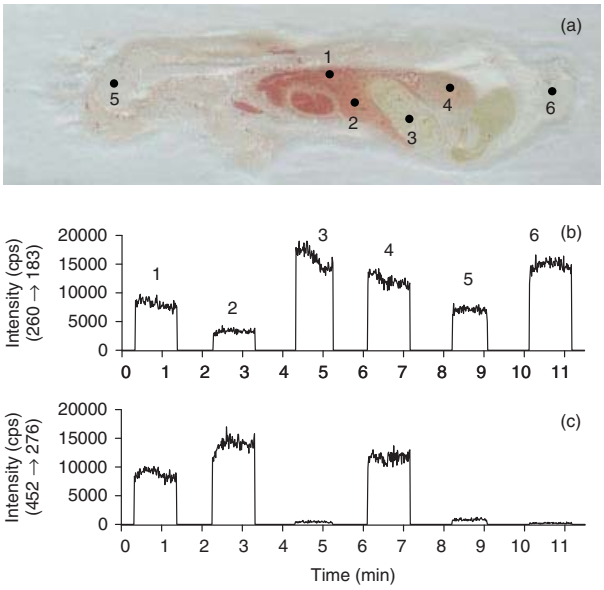

Figure 5. (a) Photograph of a propranolol dosed mouse (7.5 mg/kg, I.V. dosed, sacrificed 1 h after dose) whole-body thin tissue section showing six discrete points analyzed using the robotic nanospray system. Signal levels for (b) propranolol (m/z 260 → 183) and (c) hydroxypropranolol glucuronide (m/z 452 → 276) were recorded during 1-min spraying of samples taken at each point. Dwell time was 50 ms for each transition monitored. Extraction solvent was 80/20/0.1 (v/v/v) ACN/water/FA. Aspirated and dispensed solvent volumes were 3 and 2 µl, respectively, and aspirated sample volume was 2 µl. Sampling locations: 1 = lung; 2 = liver; 3 = stomach/contents; 4 = kidney; 5 = brain; 6 = muscle.

NanoMate system, various changes would improve the analytical performance of the device. An appropriate sample (surface) holder and solvent reservoir(s) would be of benefit for obvious reasons. Also, faster movement of the robotic arm would improve on overall sampling speed by reducing the time that is not directly spent on sampling the surface. In addition, finer control over extraction solvent flow rate when dispensing and retrieving the solution on/from the surface would allow more reproducible formation and retraction of the probe-to-surface liquid microjunction, respectively. In return, this would likely improve signal reproducibility between sample replicates. It might also enable the liquid microjunction size to be limited to the diameter of the pipette tip (~1 mm). Furthermore, the ability to select any location to sample on a surface would be beneficial. The current software only allows sampling of those locations that correspond to centers of wells of a well plate. This was sufficient for sampling of a MALDI plate insert or the punched dried blood spots, but proved inconvenient when analyzing the thin tissue sections. These simple advancements would improve not only the analysis applications demonstrated here but would certainly enhance the analysis of other analytically important surfaces.

Acknowledgements

Marissa Vavrek and Kenneth A. Koeplinger (Merck Research Laboratories, West Point, PA, USA) are thanked for the whole-body mouse thin tissue sections. Neil Spooner and Paul Abu-Rabie (GlaxoSmithKline, Ware, UK) are thanked for supplying the dried blood spot samples. Simon Prosser (Advion) is thanked for access to and assistance with the Advanced User Interface of the ChipSoftManager software. The study of the surface sampling fundamentals using the nanoelectrospray system employed here was supported by the Division of Chemical Sciences, Geosciences and Biosciences, Office of Basic Energy Sciences, United States Department of Energy. Investigation of the particular analytical surfaces reported was funded by the Battelle Memorial Institute Technology Maturation Fund. Oak Ridge National Laboratory is managed by UT-Battelle, LLC for the US Department of Energy under contract DE-AC05-00OR22725.

Supporting information

Supporting information may be found in the online version of this article.

References

[1] G. J. Van Berkel, S. P. Pasilis, O. Ovchinnikova. Established and emerging atmospheric pressure surface sampling/ionization techniques for mass spectrometry. *J. Mass Spectrom.* **2008**, *43*, 1161.
[2] G. A. Harris, L. Nyadong, F. Fernandez. Recent developments in ambient ionization techniques for analytical mass spectrometry. *Analyst* **2008**, *133*, 1297.
[3] A. Venter, M. Nefliu, R. G. Cooks. Ambient desorption ionization mass spectrometry. *Trends Anal. Chem.* **2008**, *27*, 284.
[4] T. Wachs, J. Henion. Electrospray device for coupling microscale separations and other miniaturized devices with electrospray mass spectrometry. *Anal. Chem.* **2001**, *73*, 632.
[5] G. J. Van Berkel, A. D. Sanchez, J. M. E. Quirke. Thin-layer chromatography and electrospray mass spectrometry coupled using a surface sampling probe. *Anal. Chem.* **2002**, *74*, 6216.
[6] T. Wachs, J. Henion. A device for automated direct sampling and quantitation from solid-phase sorbent extraction cards by electrospray tandem mass spectrometry. *Anal. Chem.* **2003**, *75*, 1769.
[7] M. J. Ford, G. J. Van Berkel. An improved thin-layer chromatography/mass spectrometry coupling using a surface sampling probe electrospray ion trap system. *Rapid Commun. Mass Spectrom.* **2004**, *18*, 1303.
[8] M. J. Ford, V. Kertesz, G. J. Van Berkel. Thin layer chromatography/electrospray ionization triple quadrupole linear ion trap mass spectrometry system: analysis of rhodamine dyes separated on reversed-phase C8 plates. *J. Mass Spectrom.* **2005**, *40*, 866.
[9] M. J. Ford, M. A. Deibel, B. A. Tomkins, G. J. Van Berkel. Quantitative thin-layer chromatography/mass spectrometry analysis of caffeine using a surface sampling probe electrospray ionization tandem mass spectrometry system. *Anal. Chem.* **2005**, *77*, 4385.
[10] K. G. Asano, M. J. Ford, B. A. Tomkins, G. J. Van Berkel. Self-aspirating atmospheric pressure chemical ionization source for direct sampling of analytes on surfaces and in liquid solutions. *Rapid Commun. Mass Spectrom.* **2005**, *19*, 2305.
[11] V. Kertesz, M. J. Ford, G. J. Van Berkel. Automation of a surface sampling probe/electrospray mass spectrometry system. *Anal. Chem.* **2005**, *77*, 7183.
[12] G. J. Van Berkel, M. J. Ford, M. J. Doktycz, S. J. Kennel. Evaluation of a surface sampling probe electrospray mass spectrometry system for the analysis of surface deposited and affinity captured proteins. *Rapid Commun. Mass Spectrom.* **2006**, *20*, 1144.
[13] G. J. Van Berkel, V. Kertesz, K. A. Koeplinger, M. Vavrek, A. T. Kong. Liquid micro-junction surface sampling probe electrospray mass spectrometry for detection of drugs and metabolites in thin tissue sections. *J. Mass Spectrom.* **2008**, *43*, 500.
[14] V. Kertesz, G. J. Van Berkel, M. Vavrek, K. A. Koeplinger, B. B. Schneider, T. R. Covey. Comparison of drug distribution images from whole-body thin tissue sections obtained using desorption electrospray ionization tandem mass spectrometry and sutoradiography. *Anal. Chem.* **2008**, *80*, 5168.
[15] G. J. Van Berkel, V. Kertesz. Electrochemically initiated tagging of thiols using an electrospray ionization-based liquid microjunction surface sampling probe two-electrode cell. *Rapid Commun. Mass Spectrom.* **2009**, *23*, 1380.

[16] G. J. Van Berkel, V. Kertesz, R. C. King. High throughput mode liquid microjunction surface sampling probe. *Anal. Chem.* **2009**, *821*, 7096.
[17] G. A. Schultz, T. N. Corso, S. J. Prosser, S. Zhang. A fully integrated monolithic microchip electrospray device for mass spectrometry. *Anal. Chem.* **2000**, *72*, 4058.
[18] S. Zhang, C. K. Van Pelt, D. B. Wilson. Quantitative determination of noncovalent binding interactions using automated nanoelectrospray mass spectrometry. *Anal. Chem.* **2003**, *75*, 3010.
[19] K. Geddes, G. Adamson, N. Dube, S. Crathern, R. C. King. Semi-automated tandem mass spectrometric (MS/MS) triple quadrupole operating parameter optimization for high-throughput MS/MS detection workflows. *Rapid Commun. Mass Spectrom.* **2009**, *23*, 1303.
[20] Infusion mode of the NanoMate system. http://www.advion.com/biosystems/triversananomate/flash/mode 1.htm. [Last accessed: 27 November 2009].
[21] G. J. Van Berkel, V. Kertesz. Application of a liquid extraction based sealing surface sampling probe for mass spectrometric analysis of dried blood spots and mouse whole-body thin tissue sections. *Anal. Chem.* **2009**, *81*, 9146.
[22] J. Gobey, M. Cole, J. Janiszewski, T. Covey, T. Chau, P. Kovarik, J. Corr. Characterization and performance of MALDI on a triple quadrupole mass spectrometer for analysis and quantification of small molecules. *Anal. Chem.* **2005**, *77*, 5643.
[23] P. Hatsis, S. Brombacher, J. Corr, P. Kovarik, D. A. Volmer. Quantitative analysis of small pharmaceutical drugs using a high repetition rate laser matrix-assisted laser/desorption ionization source. *Rapid. Commun. Mass Spectrom.* **2003**, *17*, 2303.
[24] L. Sleno, D. A. Volmer. Some fundamental and technical aspects of the quantitative analysis of pharmaceutical drugs by matrix-assisted laser desorption/ionization mass spectrometry. *Rapid Commun. Mass Spectrom.* **2005**, *19*, 1928.
[25] J. J. Corr, P. Kovarik, B. B. Schneider, J. Hendrikse, A. Loboda, T. R. Covey. Design considerations for high speed quantitative mass spectrometry with MALDI ionization. *J. Am. Soc. Mass Spectrom.* **2006**, *17*, 1129.
[26] V. P. Shah, K. K. Midha, J. W. A. Findlay, H. M. Hill, J. D. Hulse, I. J. McGilveray, G. McKay, K. J. Miller, R. N. Patnaik, M. L. Powell, A. Tonelli, C. T. Viswanathan, A. Yacobi. Bioanalytical method validation – a revisit with a decade of progress. *Pharm. Res.* **2000**, *17*, 1551.
[27] D. H. Chace. Mass spectrometry in newborn and metabolic screening: historical perspective and future directions. *J. Mass Spectrom.* **2009**, *44*, 163.
[28] D. H. Chace, T. A. Kalas, E. W. Naylor. Use of tandem mass spectrometry for multianalyte screening of dried blood specimens from newborns. *Clinical Chem.* **2003**, *49*, 1797.
[29] P. Rinaldo, S. Tortorelli, D. Matern. Recent developments and new applications of tandem mass spectrometry in newborn screening. *Curr. Opin. Pediatr.* **2004**, *16*, 427.
[30] N. Spooner, R. Lad, M. Barfield. Dried blood spots as a sample collection technique for the determination of pharmacokinetics in clinical studies: considerations for the validation of a quantitative bioanalytical method. *Anal. Chem.* **2009**, *81*, 1557.
[31] P. M. Edelbroek, J. van der Heijden, L. M. L. Stolk. Dried blood spot methods in therapeutic drug monitoring: methods, assay, and pitfalls. *Ther. Drug Monit.* **2009**, *31*, 327.
[32] E. G. Solon, S. K. Balani, F. W. Lee. Whole-body autoradiography in drug discovery. *Curr. Drug Metab.* **2002**, *3*, 451.
[33] T. Sten, S. Qvisen, P. Uutela, L. Luukkanen, R. Kostiainen, M. Finel. Prominent but reverse stereoselectivity in propranolol glucuronidation by human UDP-glucuronosyltransferases 1A9 and 1A10. *Drug Metab. Dispos.* **2006**, *34*, 1488.